Research Report 15/99

HÖGSKOLAN KARLSKRONA RONNEBY

Behind Acoustic Doppler Current Profiler
- Narrowband Volume Backscattering Signal Model, Analysis and Estimation

by

Xiao-Jiao Tao, Ingvar Claesson,
Nedelko Grbic, Mikael Åsman

Department of Telecommunications
and Signal Processing
University of Karlskrona/Ronneby
S-372 25 Ronneby
Sweden

ISSN 1103-1581
ISRN HKR-RES—99/15—SE

Acoustic Doppler Current Profiler - Narrowband Volume Backscattering Signal Model, Analysis and Estimation

by Xiao-Jiao Tao, Ingvar Claesson, Nedelko Grbic, Mikael Åsman

ISSN 1103-1581
ISRN HKR-RES—99/15—SE

Printed by Psilander Grafiska, Karlskrona 1999

Behind Acoustic Doppler Current Profiler

– Narrowband Volume Backscattering Signal Model, Analysis and Estimation

Xiao-Jiao Tao Ingvar Claesson
Nedelko Grbić Mikael Åsman

September 1999

Research Report 09/99
Department of Telecommunications and Signal Processing
University of Karlskrona/Ronneby, Sweden

Abstract

This report examines the statistical properties of the narrowband Doppler volume backscattering process and discusses its spectral centroid estimation problem. After clarifying the mechanism of both the finite duration Doppler effect and the continuously space-shifted integration process, the first two order time-varying statistics under a more general assumption, i.e. von Mises distribution, of random phase are derived. The generalization permits nonuniform phase tendency, which occurs in layered medium scattering. Based on the locally stationary process model, the evolutionary spectrum of the signal is derived where the variation of the backscattering strength enters as an amplitude modulation. On the contrary, the variation of the random phase distribution acts as both the amplitude modulation and the frequency modulation. The observability and the estimation of the average flow speed are discussed. It is shown that even under the homogeneous condition, the spectral centroid does not coincide with the average flow speed. Finally, a semiparametric spectral centroid estimation method, which simply contains an AR(2) model with its time-varying coefficients adapted by a wavelet shrinkage is proposed.

Contents

Chapter 1

Introduction

The narrowband acoustic Doppler volume backscattering technique has been used extensively for measuring current-speed profiles and for observing physical and biological processes within the ocean. Basically, a high-frequency narrowband acoustic beam is transmitted to illuminate the scatterers, i.e. the suspended particles in the water, like plankton and air bubbles. The physical characteristics of these scatterers will cause certain modifications in the backscattering signal, for instance, attenuation in amplitude and Doppler shift in frequency [1][2]. Thus, from the received backscattering signal, information about such factors as size, type, distribution and speed of the scatterers may be extracted. Furthermore, if their motion is mainly driven by the ocean currents, the "average" speed profile of the flow can be estimated [5] [6]. Compared with the predominant rotor and vane or propeller-type mechanical instruments, the major attraction of the acoustic Doppler current profiler (ADCP) is its remote measuring capability, i.e. in situ measuring without disturbing the velocity field of interest. This advantage has caused a progression to the latter type of ocean current measurement in the last few years [7].

Despite the expanded interest and application of this technique, there are still many problems that need further study. First of all, since the narrowband burst signal sent out to observe the Doppler effect has practically finite duration, frequency is clearly not the only parameter that has been changed. Secondly, the volume backscattering process also implies an important feature of the received signal, that is, a continuously space-shifted integration of the random signal components contributed by the different scatterers. Therefore, it is essential to create a model to characterize these physical properties of the volume backscattering process. Otherwise, it is rather difficult to answer questions as to what has really been measured, what are the required conditions, etc. Finally, although it is well known that an acoustic Doppler backscattering signal has a dynamic structure, most of the past studies regarding the system performance and estimation methods have been restricted to the unrealistic stationary signal model.

The first aim of this work is to formulate the narrowband acoustic Doppler volume backscattering process, and analyze its features based on the model. Beginning with the basic properties of the finite duration Doppler effect, we propose a general signal model for the volume backscattering process under a more general random phase assumption, i.e. the von Mises probability distribution. This model takes both the finite duration Doppler effect and the continuously space-shifted integration into consideration. Following the first two order time-varying statistical structures of the signal model, the evolutionary spectrum expression of the backscattering signal is derived on the basis of a locally stationary model introduced by Dahlhaus [14]. The role of backscattering strength and random phase distribution in the evolutionary spectrum is also addressed. Finally, we discuss the observability of the "average" flow velocity. It is shown that the spectral centroid does coincide with the "average"flow velocity under certain conditions.

The second aim is to propose the corresponding time-varying spectral centroid estimation method. Directly from the previous analysis, the backscattering signal is simplified as an amplitude-frequency modulated signal model (AFM). A semiparametric approach is constructed by an autoregressive process (AR) of order two, with its time-varying coefficients ideally adapted by the wavelet shrinkage. The reason of the construction lies in three aspects: 1. the time-varying AR model has been shown to be a locally stationary process [14]. 2. using the parametric model AR(2) to approximate the AFM at any time instant results in high accuracy gained by the underlying linear prediction function of the AR model. 3. using the nonparametric wavelet shrinkage can optimally, in minimax sense, adapt the unknown temporal variation of both amplitude modulation (AM) and frequency modulation (FM).

Both the simulated data and that collected at the Hong Kong of China and Turbaden of Sweden, with Hytec AB's ADCM-300 acoustic Doppler current profiler, are used for illustrating the analytic results and testing the performance of the proposed algorithm.

The report is organized as follows. Chapter 2 discusses the basic properties of the narrowband Doppler volume backscattering signal model. Chapter 3 analyzes its spectral properties based on the locally stationary model, and studies relevant observability and estimation issues. Chapter 4 details the estimation algorithm. Chapter 5 presents the simulation results. Finally, conclusions are drawn in Chapter 6.

Chapter 2

Properties of the Doppler Volume Backscattering Process

The Doppler effect is one of the most apparent influences of relative motion between source, medium and observer. In addition to the well-known frequency shift effect [3], however, there also exists other features including the duration shift, the density shift of the volume scatterers, and the continuously space-shifted integration process. Without loss of generality, the transient response of both the transducer and scatterers is ignored in the following discussion.

2.1 The finite duration Doppler effect of a single scatterer

Consider sending out a burst signal into the water with a transducer. The signal is assumed to have a sinusoidal form,

$$b(t) = a \sin(\omega_s t + \theta_s) \tag{2.1}$$

where a, ω_s and θ_s denote the amplitude, center frequency and phase, respectively. If the scatterer is moving at a velocity v relative to the sensor, then the signal received at the sensor will have a shifted center frequency as,

$$\omega_o = \omega_s \frac{v_s + v}{v_s - v} \tag{2.2}$$

where v_s denotes the speed of sound in water. Equation (2.2) is the product between $\omega_s \frac{v_s+v}{v_s}$, which corresponds to the movement of the scatterer as observer, and $\omega_s \frac{v_s}{v_s-v}$ which is due to the scatterer's advance on its own wave crests.

Meanwhile, if the burst signal has finite duration, i.e. $t \in [0, T_s]$, then the duration of the received signal will also change. Suppose at time $t = 0$, the scatterer

is moving at velocity v from range r towards the sensor. If the transducer sends out the burst signal at the time $t = t'$, then at the time $t = t' + \frac{r-vt'}{v_s+v}$, or when the scatterer is at the range $r = v_s\frac{r-vt'}{v_s+v}$, the sound encounters the scatterer. The sensor will receive the backscattering signal from the scatterer at the time,

$$t = \frac{2r}{v_s + v} + \frac{v_s - v}{v_s + v}t' \tag{2.3}$$

From (2.3) it is clear that the duration of the received signal will be,

$$T_o = T_s\left(\frac{v_s - v}{v_s + v}\right) \tag{2.4}$$

Therefore, the relation between duration and center frequency may be written as,

$$\omega_s T_s = \omega_o T_o = c \tag{2.5}$$

where c is a constant.

It should be noted here that, with the free stream and ideal sensor assumption, the amplitude of the backscattering signal from one scatterer depends on both the scatterer's acoustical properties and the sound pressure in the medium, which are not affected by the relative motion [4]. This means that the energy contributed by the scatterer is approximately proportional to the duration, T_o, in which the scatterer exists in the sound field.

From the duality of duration and bandwidth, it is obvious that the finite duration Doppler effect causes not only the center frequency shift but also a relative change of the spectral bandwidth. For simplicity, assuming that the backscattering signal is a sinusoid with unit amplitude and finite duration, then its power spectrum is a sinc-square function modulated by the Doppler center frequency, i.e. $P(\omega) = \frac{T_o^2}{4}\text{sinc}^2\left(\frac{\omega T_o}{2} \pm c\right)$. Clearly this is an asymmetric distribution function of the Doppler frequency shift. Such effect in the positive side of the power spectrum domain is depicted in Figure 2.1, where the solid line represents the spectrum of the backscattering signal from a still scatterer with its center frequency as ω_s. The dotted line corresponds to the signal spectrum from a scatterer which is moving away from the sensor and has center frequency ω_1, and the dashed line corresponds to that from a scatterer which is moving towards the sensor and has center frequency ω_2. The figure shows that the higher the velocity v of the scatterer, the higher the Doppler frequency shift, the shorter the duration T_o, the wider the spectral bandwidth, and the lower the signal energy $\frac{T_o^2}{4}$.

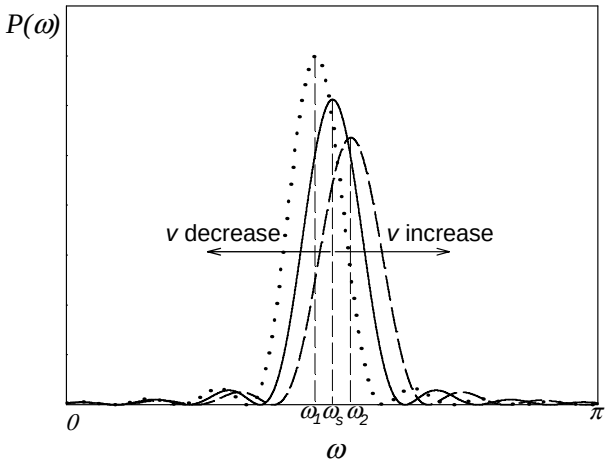

Figure 2.1: The finite duration Doppler effect of a single scatterer in power spectrum domain. Dotted line, solid line and dashed line denote the power spectrum of the backscattering signal from a scatterer with negative, zero and positive velocity towards the sensor, respectively. Their corresponding center frequency are denoted as ω_1, ω_s and ω_2, repectively.

2.2 The sum of the signals from the scatterers moving with the same velocity from the same range

When scatterers are widely and randomly spaced, all of those moving with the same velocity from the same range r can be considered as one scatterer with its scattering signal as,

$$x\left(\omega_o, r, t'\right) = \begin{cases} A_{\omega_o,r} \sin\left(\omega_o t' + \varphi_r\right), & t' \in \left[-\frac{T_o}{2}, \frac{T_o}{2}\right] \\ 0, & otherwise \end{cases} \tag{2.6}$$

where $A_{\omega_o,r}$ and φ_r denote amplitude and phase of the signal, respectively. The time interval is set as $t' \in \left[-\frac{T_o}{2}, \frac{T_o}{2}\right]$ instead of $[0, T_o]$, with the purpose of centralizing both the average location of the moving scatterer and its contribution to the final receiving signal.

The random phase φ_r is commonly taken to be uniformly distributed on the interval $[-\pi, \pi]$, implying no tendency of particular phase. However, such a situation might occur, where certain phase is favored. For example, when acoustic radiation is scattered off from a layered medium where the variance of layer roughness is small compared with the incident wavelength. In the present report, the phases are generally assumed to have an independent and possibly nonuniform distribu-

tion over the basic interval $[-\pi, \pi]$, governed by the von Mises probability density function (PDF).

Assumption 1: The probability density function (PDF) of the random phase φ_r is assumed to be a von Mises distribution,

$$f(\varphi_r) = \begin{cases} e^{\zeta_r \cos(\varphi_r - \bar{\varphi}_r)} \left[2\pi I_0(\zeta_r)\right]^{-1}, & |\varphi_r - \bar{\varphi}_r| \leq \pi \\ 0, & |\varphi_r - \bar{\varphi}_r| > \pi \end{cases} \tag{2.7}$$

where ζ_r is a real non-negative parameter and $I_0(\zeta_r)$ is the first kind modified Bessel function of order zero. The phase mean is denoted as $\bar{\varphi}_r$.

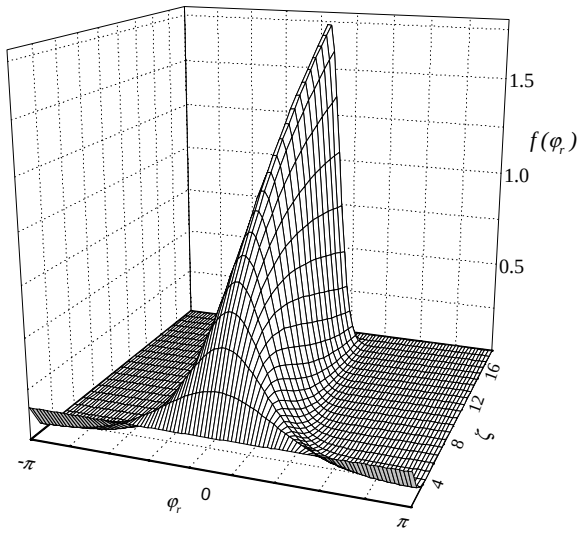

Figure 2.2: von Mises probability distribution of phase:
$f(\varphi_r) = e^{\zeta_r \cos(\varphi_r - \bar{\varphi}_r)}[2\pi I_0(\zeta_r)]^{-1}$, where $\bar{\varphi}_r = 0$.

The von Mises PDF contains two special cases, a uniform distribution when $\zeta_r = 0$, while a Gaussian distribution when $\zeta_r \to \infty$, see figure 2.2. When $\zeta_r = 0$, then $I_0(0) = 1$, and Equation (2.7) reduces to the usual uniform distribution on interval $[-\pi, \pi]$. At the other extreme of very large ζ_r, $f(\varphi_r)$ is approximately a Gaussian distribution with mean $\bar{\varphi}_r$ and variance ζ_r^{-1}. Thus, the introduction of von Mises PDF into the model allows a versatile and more accurate treatment of the problem.

In viewing the amplitude $A_{\omega_o,r}$ as the phasor summation of the random backscatterer coefficients of each individual scatterer inside a "resolution cell", many statistical models have been proposed for analysis of the amplitude (or envelope) of the backscattered signal, including Rayleigh distribution (the ideal model required high scatterer density condition) [8] [9], Rice distribution (the model to account for

non-random coherent component of the backscattered signal) [10] [11], K distribution (the generalized model to account for non-uniformity in scatterer distribution) [12] and other mixture versions of them [13]. However, it is rather difficult to apply these approaches to the volume scattering where the burst signal has a finite duration and there exists a spatial overlapping of the signal components from the different scatterers even within the resolution cell. In this report, a deterministic treatment of the amplitude is utilized: by assuming an unknown but bounded smoothness of the amplitude $A_{\omega_o,r}$, the time-varying spectrum of backscattering signal can be defined (in section III) and the spatial distribution of amplitude can be resolved simultaneously.

2.3 The density shift of the volume scatterers

As with the duration, the number of scatterers covered by the sound propagation at any time instant, or the equivalent density of the scatterers observed at the sensor, will change with the relative motion. Assume that all the scatterers in the range interval $[r, r+\Delta r]$ move at the same velocity v towards the sensor, and their density is defined as $D = \Delta n/\Delta r$, where Δn denotes the number of the scatterers in the range interval. As described in (2.3), at the sensor the time difference between the arrival of the signal from range r and that from $r + \Delta r$ is,

$$\Delta t = \frac{2\Delta r}{v_s + v} \tag{2.8}$$

and the range difference observed is,

$$\Delta r' = v_s \frac{\Delta t}{2} = \frac{v_s}{v_s + v} \Delta r \tag{2.9}$$

Therefore, the equivalent density of the scatterers observed at the sensor becomes,

$$D' = \frac{\Delta n_b}{\Delta r} = \frac{v_s + v}{v_s} D \tag{2.10}$$

The density shift rises up a question regarding the *a prior* statistical distribution assumption of the amplitude $A_{\omega_o,r}$. The unknown relative motion compresses or expands the (unknown) dynamic coordinate r as the (observed) static coordinate $r' = r\frac{v_s}{(v_s+v)}$, and from (2.10) we have

$$A^2_{\omega_o,r'} = \frac{v_s + v}{v_s} A^2_{\omega_o,r} = \frac{2\omega_o}{\omega_s + \omega_o} A^2_{\omega_o,r} \quad . \tag{2.11}$$

or equivalently,

$$\begin{aligned}\int_0^r A_{\omega_o,r}^2 dr &\overset{r=\frac{v_s+v}{v_s}r'}{\Longrightarrow} \int_0^{r'} \frac{v_s+v}{v_s} A_{\omega_o,r}^2 dr' \\ &\overset{r'=2v_s t}{\Longrightarrow} \int_0^t 2\left(v_s+v\right) A_{\omega_o,r}^2 dt \\ &= \int_0^t \frac{4\omega_o v_s}{\omega_o+\omega_s} A_{\omega_o,r}^2 dt \end{aligned} \tag{2.12}$$

With respect to which coordinate the amplitude assumption is more appropriate? To answer this question still needs further investigation. However, we will show that, in Chapter 3, no matter which coordinate is chosen, there exists an intrinsic bias term in the frequency centriod estimate.

2.4 The continuously space-shifted integration process

At any time instant t, the received backscattering signal component $y(\omega_o, t)$ will be a spatially shifted integration of those signal subcomponents $x\left(\omega_o, r, t'\right)$ that satisfy the constraint $t = 2r/(v_s+v) + t'$, as illustrated in figure 2.3.

Since $t' \in \left[-\frac{T_o}{2}, \frac{T_o}{2}\right]$, the integration interval is inversely proportional to the Doppler frequency. This mechanism may be formulated as,

$$\begin{aligned} y\left(\omega_o, t\right) &= \int_{r_1}^{r_2} x\left(\omega_o, r, t'\right) dr \\ &= \int_{r_1}^{r_2} A_{\omega_o,r} \sin\left(\omega_o t' + \varphi_{\omega_o,r}\right) dr \end{aligned} \tag{2.13}$$

where $r_1 = \left(t - \frac{T_o}{2}\right)\left(v_s+v\right)/2$, and $r_2 = \left(t + \frac{T_o}{2}\right)\left(v_s+v\right)/2$. Transforming the dynamic coordinate r first to the static coordinate r' then to the time coordinate yields a new constraint $t = 2r'/v_s + t'$ and,

$$y\left(\omega_o, t\right) = 2\sqrt{\frac{v_s\omega_o}{\omega_s+\omega_o}} \int_{-\frac{T_o}{2}}^{\frac{T_o}{2}} A_{\omega_o,t-t'} \sin\left(\omega_o t' + \varphi_{\omega_o,t-t'}\right) dt' \tag{2.14}$$

Finally, after one more integration of (2.14) over ω_o, the Doppler volume backscattering signal is given as,

$$z\left(t\right) = 2\int_{-\infty}^{\infty} \sqrt{\frac{v_s\omega_o}{\omega_s+\omega_o}} \int_{-\frac{T_o}{2}}^{\frac{T_o}{2}} A_{\omega_o,t-t'} \sin\left(\omega_o t' + \varphi_{t-t'}\right) dt' d\omega_o + \varepsilon\left(t\right) \tag{2.15}$$

where $\varepsilon\left(t\right)$ is assumed to be an additive zero-mean white Gaussian noise, i.e. $\varepsilon\left(t\right) \sim N\left(0, \sigma_\varepsilon^2\right)$.

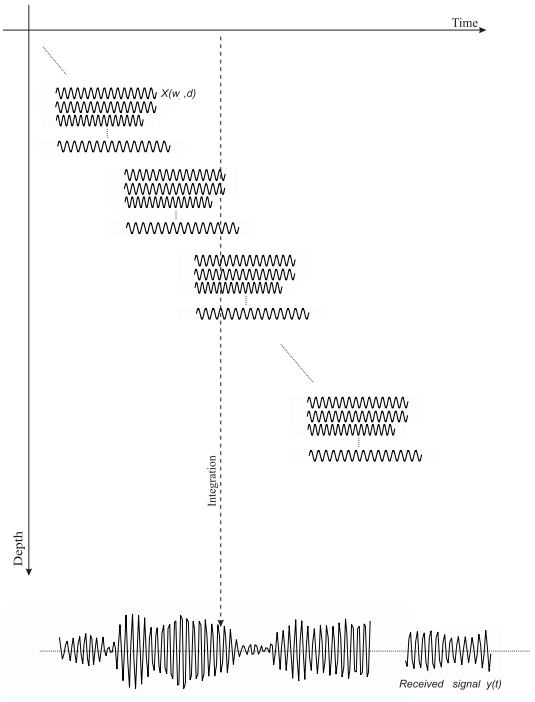

Figure 2.3: The spatially shifted integration mechanism of acoustic Doppler volume backscattering process.

2.5 The first two order time-varying statistics

From the signal model in (2.14), the mean value of $y(\omega_o, t)$ may be written as,

$$\begin{aligned} \bar{y}(\omega_o, t) &= E\{y(\omega_o, t)\} \\ &= 2\sqrt{\frac{v_s\omega_o}{\omega_s+\omega_o}}\int_{-\frac{T_o}{2}}^{\frac{T_o}{2}} A_{\omega_o,t-t'}\lambda_{t-t'}\sin\left(\omega_o t' + \bar{\varphi}_{t-t'}\right)dt' \end{aligned} \tag{2.16}$$

and the covariance function as,

$$\begin{aligned} &\operatorname{cov}\left[y\left(\omega_o, t-\frac{\tau}{2}\right), y\left(\omega_o, t+\frac{\tau}{2}\right)\right] \\ =\ & E\left\{\left[y\left(\omega_o, t-\frac{\tau}{2}\right) - \bar{y}\left(\omega_o, t-\frac{\tau}{2}\right)\right]\left[y(\omega_o, t+\frac{\tau}{2}) - \bar{y}(\omega_o, t+\frac{\tau}{2})\right]\right\} \\ =\ & \cos(\omega_o|\tau|)\int_{-\frac{T_o-|\tau|}{2}}^{\frac{T_o-|\tau|}{2}} A^2_{\omega_o,t-t'}\kappa_{t-t'}dt'\frac{2v_s\omega_o}{(\omega_s+\omega_o)} \\ &+\int_{-\frac{T_o-|\tau|}{2}}^{\frac{T_o-|\tau|}{2}} A^2_{\omega_o,t-t'}\rho_{t-t'}\cos\left(2\omega_o t' + 2\bar{\varphi}_{t-t'}\right)dt'\frac{2v_s\omega_o}{\omega_s+\omega_o}, \\ &\qquad\qquad \tau\in[-T_o, T_o] \end{aligned} \tag{2.17}$$

with

$$\begin{aligned}\lambda_{t-t'} &= I_1(\zeta_{t-t'})\, I_0(\zeta_{t-t'})^{-1} \\ \kappa_{t-t'} &= 1-\lambda_{t-t'}^2 \\ \rho_{t-t'} &= \lambda_{t-t'}^2 - I_2(\zeta_{t-t'})\, I_0(\zeta_{t-t'})^{-1}\end{aligned} \tag{2.18}$$

where $I_k(\zeta_{t-t'})$ $(k=0,1,2)$ denotes the first kind modified Bessel function of order k. Three parameters $\lambda_{t-t'}$, $\kappa_{t-t'}$ and $\rho_{t-t'}$ are non-negative functions of ζ, see figure 2.4. When $\zeta_{t-t'}=0$, i.e. the random phase has a uniform distribution, and $\lambda_{t-t'}=0$, the signal has zero mean. Meanwhile, as $\kappa_{t-t'}=1$ and $\rho_{t-t'}=0$, there exists only one nonzero term in (2.17), which contains information about the backscattering strength. The reader is referred to Appendix A for the detailed derivation of (2.16) and (2.17).

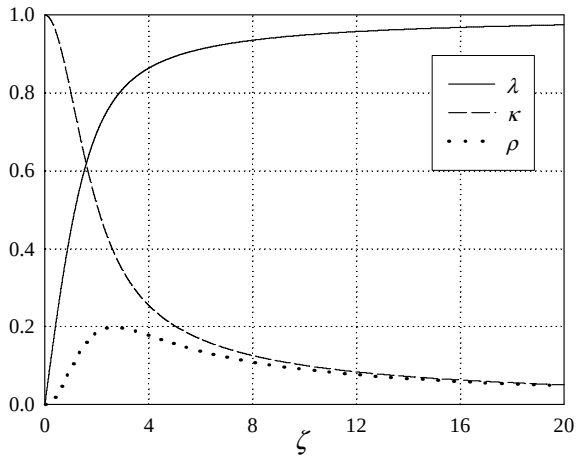

Figure 2.4: The relation of the three functions with ζ.
Solid line: $\lambda = I_1(\zeta)\, I_0(\zeta)^{-1}$, Dashed line:$\kappa = 1-\lambda^2$, and Dotted line: $\rho = \lambda^2 - I_2(\zeta)\, I_0(\zeta)^{-1}$

Chapter 3

Spectral Analysis

As discussed in the preceding part, narrowband Doppler volume backscattering process is a nonstationary stochastic process. For this type of time-varying problem the ergodic hypothesis is no longer valid, and the ensemble average cannot be replaced by the time average. Unfortunately, the statistical equivalent conditions required for a rigorously theoretic analysis are very difficult to achieve in this application. For instance, by using a broadband scheme one might obtain subband data at any time instant in order to capture the dynamic structure, but the acoustic properties of the backscatterers would vary with different frequency bands as well.

In our approach, we adopt the definition of evolutionary spectrum, an extension of the Wigner-Ville spectrum based on an underlying locally stationary model [14]. It allows for both the unique definition and the consistent estimation of what might be called the spectrum of a nonstationary time series at a single point.

3.1 The locally stationary process model

Dahlhaus introduced a model, the so-called locally stationary process, which allows certain departure from stationarity and generalizes the Cramér representation of a stationary stochastic process. The reader is refered to [14] for details.

Definition 1 *A sequence of stochastic process* $\{X_{t,T}\}_{t=1,\cdots,T}$ *is called locally stationary, with transfer function* A^o *and trend* μ*, if there exists a representation*

$$X_{t,T} = \mu\left(\frac{t}{T}\right) + \int_{-\pi}^{\pi} A^o_{t,T}(\omega)\, e^{i\omega t} d\xi(\omega), \tag{3.1}$$

where:

1. $\xi(\omega)$ is a stochastic process on $[-\pi, \pi]$ with $\bar{\xi}(\omega) = \xi(-\omega)$, $E\xi(\omega) = 0$ and orthonormal increments, i.e. $\operatorname{cov}(d\xi(\omega), d\xi(\omega')) = \delta(\omega - \omega')\, d\omega$, $cum\{d\xi(\omega_1), \cdots,$

$d\xi(\omega_k)\} = \eta\left(\sum_{j=1}^{k}\omega_j\right) h_k(\omega_1,\cdots,\omega_{k-1})\, d\omega_1\cdots d\omega_k$, where $cum\{\cdots\}$ denotes the cumulant of order k, $|h_k(\omega_1,\cdots,\omega_{k-1})| \leq constant_k$ for all k (with $h_1 = 0$, $h_2(\omega) = 1$) and $\eta(\omega) = \sum_{j=-\infty}^{\infty}\delta(\omega + 2\pi j)$ is the period 2π extension of the Dirac delta function, and,

2. there exists a positive constant K and a smooth function $A(u,\omega)$ on $[0,1]\times[-\pi,\pi]$ which is 2π periodic in ω, with $A(u,\omega) = A(u,-\omega)$, such that for all T, $\sup_{t,\omega}\left|A^o_{t,T}(\omega) - A(t/T,\omega)\right| \leq KT^{-1}$. $A(u,\omega)$ and $\mu(u)$ are assumed to be continuous in u.

This model contains two parts. First, there is a rescaling in time ($u = t/T$); its purpose is to model the nonstationary time series in a way which allows an asymptotic inference on its second order structure from a single realization. Without this allowance, it is impossible to make any statistical inferences on a time-varying spectrum which depends on a growing number of time points $t = 1,\cdots,T$. The second part is an assumption of the smoothness of A in u. This condition bounds the complexity of $A(t/T,\omega)$ even when T tends to infinity. The total effect is that, when T increases, the amount of statistical information also increases by a growing number of observations. Moreover, if μ and A do not depend upon t and T, then X does not depend on T either and the spectral representation of an ordinary stationary process is obtained. Thus, the classical theory for stationary processes is a special case of this approach.

Definition 2 *The evolutionary spectrum of* $\{X_{t,T}\}_{t=1,\cdots,T}$ *given in (3.1) is defined as, for* $u \in (0,1)$,

$$f(u,\omega) = |A(u,\omega)|^2 \tag{3.2}$$

If $A(u,\omega)$ is differentiable in u and ω with uniformly bounded derivatives, then for all $u \in (0,1)$, as $T \to \infty$,

$$\int_{-\pi}^{\pi} |f_T(u,\omega) - f(u,\omega)|^2\, d\omega = o(1) \tag{3.3}$$

where

$$f_T(u,\omega) = \frac{1}{2\pi}\sum_{s=-\infty}^{\infty} \mathrm{cov}\left\{X_{uT-s/2}; X_{uT+s/2}\right\} e^{-i\omega s} \tag{3.4}$$

$X_{t,T}$ are given by (3.1), with $A^o_{t,T}(\omega) = A(0,\omega)$ for $t < 1$ and $A^o_{t,T}(\omega) = A(1,\omega)$ for $t > T$. For fixed T, $f_T(u,\omega)$ is similar to the Wigner-Ville spectrum. When $T \to \infty$, its limit form is given as $f(u,\omega)$ in mean-square sense. The inherent advantage of the locally stationary approach is that, under the smoothness assumption on $A(u,\omega)$, the definition 2 turns out to be unique.

3.2 The evolutionary spectrum of the volume backscattering process

In our application, the continuity and viscosity of the medium generally provide such necessary conditions as both the limit and the smoothness of the variations of the medium. Therefore, the Doppler volume backscattering process (2.15) may be formulated as the aforementioned locally stationary model, with time-varying trend as,

$$\begin{aligned}
\mu\left(\frac{t}{T}\right) &= \bar{z}\left(\frac{t}{T}\right) \\
&= \int_{-\infty}^{\infty} \bar{y}\left(\omega_o, \frac{t}{T}\right) d\omega_o \\
&= \int_{-\infty}^{\infty} 2\sqrt{\frac{v_s\omega_o}{\omega_s+\omega_o}} \int_{-\frac{T_o}{2}}^{\frac{T_o}{2}} A_{\omega_o,t-t'}\lambda_{t-t'} \sin\left(\omega_o t' + \bar{\varphi}_{t-t'}\right) dt' d\omega_o \\
&= \int_{-\infty}^{\infty} 2\sqrt{\frac{v_s\omega_o}{\omega_s+\omega_o}} \int_{t-\frac{T_o}{2}}^{t+\frac{T_o}{2}} A_{\omega_o,t'}\lambda_{t'} \sin\left(\omega_o t - \omega_o t' + \bar{\varphi}_{t'}\right) dt' d\omega_o \\
&= \int_{-\infty}^{\infty} 2\sqrt{\frac{v_s\omega_o}{\omega_s+\omega_o}} \Big\{ \sin\omega_o t \cdot T_o^{\frac{1}{2}} \left[W_{\frac{T_o}{2}}(t) * A_{\omega_o,t}\lambda_t \cos\left(\omega_o t - \bar{\varphi}_t\right)\right] \\
&\quad - \cos\omega_o t \cdot T_o^{\frac{1}{2}} \left[W_{\frac{T_o}{2}}(t) * A_{\omega_o,t}\lambda_t \sin\left(\omega_o t - \bar{\varphi}_t\right)\right] \Big\} d\omega_o \qquad (3.5)
\end{aligned}$$

where the power-normalized window function $W_{\frac{T_o}{2}}(t) = T_o^{-\frac{1}{2}}\left[u\left(t+\frac{T_o}{2}\right) - u\left(t-\frac{T_o}{2}\right)\right]$. The asterisk * denotes convolution operation.

Conceptually, the window function $W_{\frac{T_o}{2}}(t)$ in (3.5) acts as a low-pass filter with its spectral form as $T_o^{\frac{1}{2}}\mathrm{sinc}\left(\frac{\omega T_o}{2}\right)$. Similarly, $A_{\omega_o,t}\lambda_t$ represents an amplitude modulation and $\bar{\varphi}_t$ a frequency modulation around the center frequency ω_o. Both $A_{\omega_o,t}\lambda_t \cos\left(\omega_o t - \bar{\varphi}_t\right)$ and $A_{\omega_o,t}\lambda_t \sin\left(\omega_o t - \bar{\varphi}_t\right)$ have band-pass shaped spectra with their center frequency at $\pm\omega_o$ and their bandwidths are equal to the bandwidth of $A_{\omega_o,t}\lambda_t$ plus that of $\cos\bar{\varphi}_t$. A convolution operation between them and the window function in time domain, is equivalent to a multiplication between their spectra in frequency domain. Thus, if the bandwidths of $W_{\frac{T_o}{2}}(t)$, $A_{\omega_o,t}\lambda_t$, and $\cos\bar{\varphi}_t$ are so small that in frequency domain there is no overlapped region between their spectra, then the signal mean value will be zero, i.e. $\bar{z}\left(\frac{t}{T}\right) \to 0$. This property generally holds, except in the turbulent current situation where the distributions of backscattering strength and random phase vary closely with the range.

The evolutionary spectrum of the Doppler volume backscattering process may be written as,

$$f\left(\frac{t}{T}, \omega\right) = \int_{-\infty}^{\infty} \mathrm{cov}\left[z\left(t-\tau/2\right), z\left(t+\tau/2\right)\right] e^{-i\omega\tau} d\tau$$

$$
\begin{aligned}
&= \sigma_\varepsilon^2 + \int_{-\infty}^{\infty}\int_{-\infty}^{\infty} \mathrm{cov}\left[y\left(\omega_o, t-\tau/2\right), y\left(\omega_o, t+\tau/2\right)\right] d\omega_o e^{-i\omega\tau} d\tau \\
&= \sigma_\varepsilon^2 + \int_{-\infty}^{\infty}\int_{-\infty}^{\infty} \mathrm{cov}\left[y\left(\omega_o, t-\tau/2\right), y\left(\omega_o, t+\tau/2\right)\right] e^{-i\omega\tau} d\tau d\omega_o \\
&= \sigma_\varepsilon^2 + \int_{-\infty}^{\infty} \frac{2v_s\omega_o}{(\omega_s+\omega_o)} \int_{-T_o}^{T_o} \left\{ \cos\left(\omega_o|\tau|\right) \int_{-\frac{T_o-|\tau|}{2}}^{\frac{T_o-|\tau|}{2}} A^2_{\omega_o,t-t'}\kappa_{t-t'} dt' \right. \\
&\quad \left. + \int_{-\frac{T_o-|\tau|}{2}}^{\frac{T_o-|\tau|}{2}} A^2_{\omega_o,t-t'}\rho_{t-t'} \cos\left(2\omega_o t' + 2\bar{\varphi}_{t-t'}\right) dt' \right\} e^{-i\omega\tau} d\tau d\omega_o
\end{aligned}
$$

Finally, from Appendix B, we have a concise form as,

$$
f\left(\frac{t}{T}, \omega\right) = \int_{-\infty}^{\infty} \left[P_1\left(\omega \pm \omega_o\right) + P_2\left(\omega\right)\right] d\omega_o + \sigma_\varepsilon^2 \tag{3.6}
$$

with

$$
\begin{aligned}
P_1\left(\omega\right) &= \frac{4v_s\omega_o}{\omega_s+\omega_o} \left\{ d_1 T_o^2 \mathrm{sinc}^2\left(\frac{\omega T_o}{2}\right) + 2\frac{\cos\omega T_o}{\omega} f_{1s}\left(\omega\right) + 2\frac{\sin\omega T_o}{\omega} f_{1c}\left(\omega\right) \right\} \\
P_2\left(\omega\right) &= \frac{4v_s\omega_o}{\omega_s+\omega_o} \left\{ d_2 T_o^2 \mathrm{sinc}^2\left(\frac{\omega T_o}{2}\right) + 2\frac{\cos\omega T_o}{\omega} f_{2s}\left(\omega\right) + 2\frac{\sin\omega T_o}{\omega} f_{2c}\left(\omega\right) \right\} \\
f_{1s}\left(\omega\right) &= \int_{-\frac{T_o}{2}}^{0} \left(A^2_{\omega_o,t\pm t'}\kappa_{t\pm t'} - d_1\right) \sin 2\omega t' dt' \\
f_{2c}\left(\omega\right) &= \int_{-\frac{T_o}{2}}^{0} \left(A^2_{\omega_o,t\pm t'}\kappa_{t\pm t'} - d_1\right) \cos 2\omega t' dt' \\
f_{2s}\left(\omega\right) &= \int_{-\frac{T_o}{2}}^{0} \left[A^2_{\omega_o,t\pm t'}\rho_{t\pm t'} \cos\left(2\omega_o t' + 2\bar{\varphi}_{t\pm t'}\right) - d_2\right] \sin 2\omega t' dt' \\
f_{2s}\left(\omega\right) &= \int_{-\frac{T_o}{2}}^{0} \left[A^2_{\omega_o,t\pm t'}\rho_{t\pm t'} \cos\left(2\omega_o t' + 2\bar{\varphi}_{t\pm t'}\right) - d_2\right] \cos 2\omega t' dt' \\
d_1 &= \frac{1}{T_o} \int_{\frac{T_o}{2}}^{\frac{T_o}{2}} A^2_{\omega_o,t-t'}\kappa_{t-t'} dt' \\
d_2 &= \frac{1}{T_o} \int_{\frac{T_o}{2}}^{\frac{T_o}{2}} A^2_{\omega_o,t-t'}\rho_{t-t'} \cos\left(2\omega_o t' + 2\bar{\varphi}_{t-t'}\right) dt'
\end{aligned}
$$

where d_1 and d_2 are the DC components of $A^2_{\omega_o,t}\kappa_t$ and $A^2_{\omega_o,t}\rho_t \cos\left(2\omega_o t + 2\bar{\varphi}_t\right)$, respectively.

The evolutionary spectrum expression of the narrowband Doppler volume backscattering signal is important in the sense that it tells us what will be observed after sending out the burst signal into the medium, and how the output is affected by the variation of the medium. If we take the Doppler volume backscattering as a system identification problem with the medium as the system and the burst signal as the input, then (3.6) gives us the expected output. The general properties of the output are detailed as follows:

1. Two factors of the medium, the backscattering strength and random phase, enter the evolutionary spectrum differently. The backscattering strength $A^2_{\omega_o,t}$ can be taken as an amplitude modulation in both terms in (3.6). However, the distribution of the random phase, which is characterized by the parameters κ_t, ρ_t and $\bar{\varphi}_t$, is an amplitude modulation in $P_1(\omega)$, and it has both an amplitude modulation and a frequency modulation effect on $P_2(\omega)$.

2. In general, $P_2(\omega)$ is much smaller than $P_1(\omega)$, due to the fact that,

   (a) d_1 is the DC component of $A^2_{\omega_o,t}\kappa_t$ which has a lowpass spectrum, whereas d_2 is the DC component of a bandpass signal $A^2_{\omega_o,t}\rho_t \cos(2\omega_o t + 2\bar{\varphi}_t)$. Therefore $d_1 \gg d_2$.

   (b) the function $\frac{\cos \omega T_o}{\omega}$ and $\frac{\sin \omega T_o}{\omega}$ can be seen as lowpass filters, whose bandwidths are inversely proportional to the duration T_o. Since $f_{1c}(\omega)$ and $f_{1s}(\omega)$ have lowpass spectra while $f_{2c}(\omega)$ and $f_{2s}(\omega)$ have bandpass spectra, the last two terms of $P_2(\omega)$ are generally much smaller than that of $P_1(\omega)$.

3. Due to the finite duration Doppler effect, in the time domain the autocorrelation length of the backscattering signal is inversely proportional to the Doppler frequency ω_o, see (2.17). The corresponding effects in spectrum domain are:

   (a) the peak of the spectrum component contributed by $y(\omega_o, t)$ is inversely proportional to ω_o, while,

   (b) a larger ω_o yields a wider spectral spread of the component $y(\omega_o, t)$.

4. The distribution of the random phase unavoidably degrades the performance of the amplitude estimation, simply because the observation is such a mixed version, namely $A^2_{\omega_o,t}\kappa_t$. For example, when sound is scattered off a layered medium or the surface of a big scatterer like a fish, where $\zeta_t \to \infty$ so that $\kappa_t \to 0$ (see Figure 2.4), $A^2_{\omega_o,t}\kappa_t$ becomes much smaller than the true value $A^2_{\omega_o,t}$. This result is interesting because it is a common experience to receive a high-amplitude response from a layered medium but this property implies that the true amplitude should be even higher. The reason is the aforementioned space-shifted integration mechanism of the volume backscattering process.

5. The simpler forms of the evolutionary spectrum may be obtained from the examination of two special cases.

(a) The duration of the burst signal is relatively long. That is, when $T_s \to \infty$ gives $T_o \to \infty$, then $P_2(\omega) \to 0$ so that,

$$f\left(\frac{t}{T}, \omega\right) = \int_{-\infty}^{\infty} P_1(\omega \pm \omega_o)\, d\omega_o + \sigma_\varepsilon^2 \tag{3.7}$$

The advantage of the above simplification given by the large T_s is that the frequency modulation part normally caused by the variation of the random phase mean value does not exist. This special case is useful for applications where the main interest is in the backscattering strength estimation, or the spectral centroid estimation as in our case, which will be discussed in the next section.

(b) The medium is homogeneous. This special case has been commonly used as an assumption in the previous studies by many authors. Clearly, it is an ideal situation, but also too strict to apply. Homogeneous means that the random phase has a uniform distribution, thus $\zeta_t = \lambda_t = \rho_t = 0$, $\kappa_t = 1$ and $A_{\omega_o,t}$ is also invariant with time,

$$f(\omega) = \int_{-\infty}^{\infty} \frac{4 v_s A_{\omega_o}^2 T_o c}{\omega_s + \omega_o} \mathrm{sinc}^2\left(\frac{\omega \pm \omega_o}{2} T_o\right) d\omega_o + \sigma_\varepsilon^2 \tag{3.8}$$

3.3 Spectral centroid analysis

In this section we study the observability of the "average" flow speed by using the Doppler volume backscattering technique. Since the common procedure is to estimate the spectral centroid of the signal, we will examine this issue based on the preceding analysis. More precisely, our purpose is to answer the question whether or not the spectral centroid equals to the center frequency, and if so, when. In the following discussion, the background noise term is neglected.

It is well known that, given a real valued realization, the centroid of the power density spectrum $f(\omega)$ can be expressed as,

$$\omega_c = \frac{\int_0^\infty \omega f(\omega)\, d\omega}{\int_0^\infty f(\omega)\, d\omega} \tag{3.9}$$

or equivalently,

$$\omega_c = \frac{\int_0^\infty \omega f(\omega)\, d\omega}{\pi R(0)} \tag{3.10}$$

where $R(0)$ is the autocovariance of the process at time zero.

Since the spectral centroid is defined by only using the positive side spectrum, it is essential to take the spectral leakage problem into consideration. In the Doppler volume backscattering application, the long duration burst signals are normally preferred in order to sufficiently excite the medium. From the preceding section and the spectral centroid definition, we can see that there are also other advantages. First the use of the long duration burst signals leads to zero mean value, and consequently it gives higher accuracy for the autocovariance estimation. Second, it removes the random phase frequency modulation. Last, it yields less aliasing between the positive side $P_1(\omega - \omega_o)$ and the negative side $P_1(\omega + \omega_o)$.

We start with considering the ideal situation, as described in the property 5 (b) of the preceding section. Given large T_o and by substituting (3.8) into the above definition, we have,

$$\begin{aligned}
\omega_c &= \frac{\int_0^\infty \omega f\left(\frac{t}{T}, \omega\right) d\omega}{\int_0^\infty f\left(\frac{t}{T}, \omega\right) d\omega} \\
&= \frac{\int_0^\infty \omega \int_{-\infty}^\infty \frac{4v_s A_{\omega_o}^2 T_o c}{\omega_s + \omega_o} \mathrm{sinc}^2\left(\frac{\omega - \omega_o}{2} T_o\right) d\omega_o d\omega}{\int_0^\infty \int_{-\infty}^\infty \frac{4v_s A_{\omega_o}^2 T_o c}{\omega_s + \omega_o} \mathrm{sinc}^2\left(\frac{\omega - \omega_o}{2} T_o\right) d\omega_o d\omega} \\
&= \frac{\int_{-\infty}^\infty \frac{A_{\omega_o}^2 T_o}{\omega_s + \omega_o} \int_0^\infty \omega \mathrm{sinc}^2\left(\frac{\omega - \omega_o}{2} T_o\right) d\omega d\omega_o}{\int_{-\infty}^\infty \frac{A_{\omega_o}^2 T_o}{\omega_s + \omega_o} \int_0^\infty \mathrm{sinc}^2\left(\frac{\omega - \omega_o}{2} T_o\right) d\omega d\omega_o} \\
&= \frac{\int_{-\infty}^\infty \frac{A_{\omega_o}^2 \omega_o}{\omega_s + \omega_o} d\omega_o}{\int_{-\infty}^\infty \frac{A_{\omega_o}^2}{\omega_s + \omega_o} d\omega_o} \qquad (3.11)
\end{aligned}$$

The solution to (3.11) requires a further assumption about the backscattering strength $A_{\omega_o}^2$. The traditional assumption of the spectrum is taken to be a Gaussian distribution function, which ignores the difference between the static coordinate r and the dynamic coordinate $r' = t/(2v_s) = rv_s/(v_s + v)$ due to the relative motion. From (3.11), it is clear that any symmetric distribution of $A_{\omega_o}^2$ will unavoidably lead to an intrinsic bias term in the centroid estimate. Suppose that $A_{\omega_o}^2$ obeys a symmetric distribution around the true center frequency ω_r, which coincides with the "average" flow velocity, with the variance $\sigma_{A_{\omega_o}^2}^2$, we have,

$$\begin{aligned}
\mathrm{Bias}(\omega) &= \omega_c - \omega_r \\
&= \frac{\int_{-\infty}^\infty \frac{A_{\omega_o}^2 \omega_o}{\omega_s + \omega_o} d\omega_o}{\int_{-\infty}^\infty \frac{A_{\omega_o}^2}{\omega_s + \omega_o} d\omega_o} - \omega_r \\
&= \frac{\int_{-\infty}^\infty A_{\omega_o}^2 d\omega_o}{\int_{-\infty}^\infty \frac{A_{\omega_o}^2}{\omega_s + \omega_o} d\omega_o} - \omega_s - \omega_r
\end{aligned}$$

$$
\begin{aligned}
&= \frac{\omega_s+\omega_r}{\int_{-\infty}^{\infty}\frac{A_{\omega_o}^2}{1+\frac{\omega_o}{\omega_s+\omega_r}}d\omega_o}-\omega_s-\omega_r \\
&\approx \frac{\omega_s+\omega_r}{\int_{-\infty}^{\infty}A_{\omega_o}^2\left[1-\frac{\omega_o}{\omega_s+\omega_r}+\left(\frac{\omega_o}{\omega_s+\omega_r}\right)^2\right]d\omega_o}-\omega_s-\omega_r \\
&= \frac{\omega_s+\omega_r}{1+\left(\frac{\sigma_{A_{\omega_o}^2}}{\omega_s+\omega_r}\right)^2}-\omega_s-\omega_r \\
&= -\frac{\omega_s+\omega_r}{\left(\frac{\omega_s+\omega_r}{\sigma_{A_{\omega_o}^2}}\right)^2+1} \qquad (3.12)
\end{aligned}
$$

From the above it is clear that the spectral centroid generally does not coincide with the center frequency. The intrinsic bias is a negative term which decreases with variance $\sigma_{A_{\omega_o}^2}$ decreasing. In other words, the smaller spectral spread (the flow speed spread) gives the smaller bias in the centroid estimate. Although the above result is obtained with respect to the dynamic coordinate, the bias of the spectral centroid with respect to the static coordinate still exists and can be easily derived by introducing (2.11) into (3.11) with the same symmetric distribution assumption,

$$
\begin{aligned}
\text{Bias}\,(\omega) &= \omega_c-\omega_r \\
&= \frac{\int_{-\infty}^{\infty}A_{\omega_o}^2 d\omega_o}{\int_{-\infty}^{\infty}A_{\omega_o}^2\omega_o^{-1}d\omega_o}-\omega_r \\
&= \frac{1}{\int_{-\infty}^{\infty}A_{\omega_o}^2\omega_r^{-1}\frac{1}{1+\frac{\omega_o}{\omega_r}}d\omega_o}-\omega_r \\
&\approx \frac{\omega_r}{\int_{-\infty}^{\infty}A_{\omega_o}^2\left[1-\frac{\omega_o}{\omega_r}+\left(\frac{\omega_o}{\omega_r}\right)^2\right]d\omega_o}-\omega_r \\
&= \frac{\omega_r}{1+\frac{\sigma_{A_{\omega_o}^2}}{\omega_r^2}}-\omega_r \\
&= -\frac{\omega_r}{1+\frac{\omega_r^2}{\sigma_{A_{\omega_o}^2}}} \qquad (3.13)
\end{aligned}
$$

The most common medium encountered is inhomogeneous, which gives non-stationary behavior of the scattering signals. Nevertheless, by using long duration burst signal, its evolutionary spectrum can still be modelled as the simple form described in the property 5 (a) of the preceding section. The corresponding spectral centroid is formulated as,

$$
\omega_{c,\frac{t}{T}} = \frac{\int_0^{\infty}\omega f\left(\frac{t}{T},\omega\right)d\omega}{\int_0^{\infty}f\left(\frac{t}{T},\omega\right)d\omega}
$$

$$
\begin{aligned}
&= \frac{\int_0^\infty \omega \int_{-\infty}^\infty P_1(\omega-\omega_o)\, d\omega_o d\omega}{\int_0^\infty \int_{-\infty}^\infty P_1(\omega-\omega_o)\, d\omega_o d\omega} \\
&= \frac{\int_{-\infty}^\infty \int_0^\infty \omega P_1(\omega-\omega_o)\, d\omega d\omega_o}{\int_{-\infty}^\infty \int_0^\infty P_1(\omega-\omega_o)\, d\omega d\omega_o} \\
&= \frac{\int_{-\infty}^\infty \omega_o \frac{\omega_o}{(\omega_s+\omega_o)} d_1 T_o d\omega_o}{\int_{-\infty}^\infty \frac{\omega_o}{(\omega_s+\omega_o)} d_1 T_o d\omega_o} \\
&= \frac{\int_{-\infty}^\infty \frac{d_1\omega_o}{(\omega_s+\omega_o)} d\omega_o}{\int_{-\infty}^\infty \frac{d_1}{(\omega_s+\omega_o)} d\omega_o}
\end{aligned} \tag{3.14}
$$

The parameter κ_t reflects the variation of the random phase distribution, and therein the variation of the medium property. When $\kappa_t = 1$, the medium has locally homogeneous property and the spectral centroid estimate is the smoothed version on the interval $\left[r - \frac{v_s T_o}{2}, r + \frac{v_s T_o}{2}\right]$. On the contrary, when $\kappa_t \to 0$, the sound is scattered off either the layered medium or the flow sheer, and the backscattering strength also vary quickly. Thus d_1 will not be the correct weight for different Doppler frequency. In this case the "average" flow speed is not observable.

Chapter 4

Spectral centroid estimation

Based on the stationary model, the traditional spectral centroid approaches including time domain methods (covariance estimation, zero-crossing and phase-lock-loop) and frequency domain methods (first-order spectral moment estimation and peak-picking) essentially contains a step windowing the signal in the time domain [5] [6] [26] [27]. Obviously, this procedure has two drawbacks. One is that the choice of the window size is a bias-covariance tradeoff of the estimate and, therefore, a statistical validation is needed in advance. Another is that accessing the time-varying details within each segment or refining the results globally still needs post-processing.

This report proposes a novel algorithm to estimate the time-varying spectral centroid of the narrowband Doppler volume backscattering signal. It is constructed in a semiparametric way; that is, modeling parametrically the local narrowband evolutionary spectrum using an AR(2), and nonparametrically adapting its time-varying coefficients using the wavelet shrinkage. The idea is to employ the underlying linear prediction function of the AR(2) and the minimaxi optimality of the unknown smoothness adaptation of the wavelet shrinkage.

The time-varying autoregressive process (TVAR) has been widely used to model nonstationary signals. Theoretically, this model belongs to Dahlhaus locally stationary processes while its evolutionary spectrum can be characterized by its time-varying coefficients [14]. The relation between TVAR(2) and the amplitude-frequency modulated (AFM) signal model was clarified in [16]. In practice, the performance of this technique is heavily dependent on the estimation of unknown time functions of AR coefficients. The standard procedure is to expand the AR coefficients using orthogonal series, including Legendre polynomials, Chebyshev polynomials, Fourier series and B-spline [16]–[17]. The main criticism of this method lies in two aspects: First, determination of the order of the basis function becomes a critical factor. Since the form and dimensionality of these traditional bases are unknown, the use of arbitrary order basis expansion inevitably either overparameterizes or

poorly represents the model. Second, the AR coefficients are not independent of each other and have different probability distributions. Therefore, the above direct procedure may yield large approximation errors or become numerically unstable. In fact, it has been shown that the above method is sensitive to noise [16].

The proposed approach consists in a nonlinear wavelet shrinkage procedure to estimate the unknown function of time [21]. Basically, Wavelet basis is an orthonormal series generated by dilations and translations of the scaling function and wavelet function. The distinct advantage of wavelet over above traditional methods, is its ability to optimally compress the functions with both rather homogeneous smoothness over whole domain and certain inhomogeneous smoothness. If the better compress-ratio is achieved (the smaller number of coefficients is needed), the better bias-covariance trade-off of the estimators is tuned [21]. Indeed, this procedure has very broad asymptotic near-optimality properties [15].

From (3.7), the backscattering signal may be formulated as a single-component random amplitude-frequency modulated process,

$$Y_t = A_t cos(\phi_t) + \epsilon_t, \qquad (t = 1, \cdots, N) \tag{4.1}$$

where Y_t, A_t and ϕ_t represent the received signal, instantaneous amplitude and phase, respectively. Both A_t and ϕ_t consist of a stationary Gaussian process and a time-varying mean value, while ϵ_t is a stationary Gaussian white noise, $\epsilon_t \sim N(0, \sigma^2)$. Then the corresponding TVAR(2) model may be written as,

$$Y_t = X_t + \epsilon_t, \tag{4.2}$$

and

$$X_t + a_{t,1} X_{t-1} + a_{t,2} X_{t-2} = \delta_t, \qquad (t = 1, \cdots, N) \tag{4.3}$$

where the input of the AR(2), δ_t, is assumed to be a stationary Gaussian white process independent of noise ϵ_t. The relation between TVAR(2) and AFM model can be described as,

$$\begin{cases} a_{t,1} &= -2c_t d_t, \\ a_{t,2} &= d_t d_{t-1}. \\ c_t &= cos(\omega_t), \\ d_t &= A_t / A_{t-1}. \end{cases} \tag{4.4}$$

where ω_t denotes the instantaneous frequency of the signal. Note that d_t corresponds to the radial movement of the AR pole whereas c_t represents the circumferential movement of the pole.

From equation (4.4), it is clear that $a_{t,1}$ and $a_{t,2}$ are dependent of each other and their probability distribution functions are different. In practice, due to the division operation in equation (4.4) and the unknown random distribution of the amplitude, the direct orthogonal series expansion of the AR coefficients may results

in numerical instabilities under low signal-to-noise ratio (SNR) conditions. In fact, it has been shown that the above method is sensitive to noise [16]. In underwater application the maximum flow speed is often rather small compared with the sound speed, for instance 0.3%, the resulting bandwidth is rather small as well. Therefore, we can always use such bandwidth information to set the amplitude modulation parameter d_t to a fix value.

Substituting d_t in equation (4.4), the frequency estimate can be found from equations (4.2) and (4.3) by using standard methods, like least-square estimation. However, it is well known that Prony's least-square estimator of the AR parameters becomes severely biased and inconsistent at low SNR. Instead, the proposed algorithm uses an Iterative Filtering scheme (IF), which was originally discussed by S. Kay [18] and generalized by T. Li [19], to solve these problems. The idea is to judiciously parameterize the filter according to the correlation structure of the noise. The frequency estimate obtained from the algorithm has exactly the same asymptotic variance as that given by Whittle's method, which is known to yield the most accurate frequency estimates [20]. Once the least-square estimate, $\hat{c}_t$, is obtained, applying it to filter the noisy signal yields the filtered process, $Y_t(\hat{c}_t)$. Then, the least-square estimation of $\hat{c}_t$ from $Y_t(\hat{c}_t)$ and filtering the original signal through $\hat{c}_t$ are repeated iteratively, until convergence is reached.

The proposed algorithm is defined as follows,

1. Set d_t and $k = 0$.

2. Solve equation $A\beta = b$ by Singular Value Decomposition (SVD) to get the least square estimates $\hat{\beta}_{LS}$, where $b = Y_t + \hat{d}_t^2 Y_{t-2}$, $A = diag(2\hat{d}_t Y_{t-1})B$, the wavelet coefficients $\hat{\beta} = B^T \hat{c}_t{}^k$ and B is a matrix whose space is spanned by wavelets bases.

3. After shrinking the wavelets coefficients $\hat{\beta}_{LS}$, the minimax estimation of $\hat{c}_t{}^k$ is given as $\hat{c}_t{}^k = B\hat{\beta}$, where $\hat{\beta}$ is the wavelet shrinkage estimate of $\hat{\beta}_{LS}$.

4. if $|\hat{c}_t{}^k - \hat{c}_t{}^{k-1}| \leq \xi$ (ξ is a small positive number, for example, $\xi = 0.0001$), go to step 6; otherwise, go to next step.

5. Using $\hat{c}_t{}^k$ filter the original data Y_t, to get the filtered version $Y_t(\hat{c}_t{}^k)$; k=k+1, goto step 2.

6. The frequency estimation is, $\hat{w}_t = cos^{-1}(\hat{c}_t{}^k)$.

It should be noted that CDJV wavelets on interval $[0, 1]$, is implemented in the above algorithm. See [23] for details.

Chapter 5

Simulation

5.1 Monte-Carlo Comparison of four algorithms

Consider the discrete FM signal,

$$Y(t) = cos(\theta t + \omega_m \sum_{i=1}^{t} cos(\omega_f i)) + \epsilon_t, \qquad (t = 1, \cdots, 514)$$

where $\theta = \pi/6$, $\omega_m = 0.5\theta$, $\omega_f = \pi/128$, and ϵ_t is a stationary white Gaussian noise, i.e. $\epsilon_t \sim N(0, \sigma^2)$. For the purpose of Monte-Carlo simulation, 5000 simulation runs have been performed for each case. A comparison of the bias and variance of estimation using four different methods, including energy operator [22], Hilbert Transform, TVAR using Chebyshev basis (order 26) and the proposed algorithm, is shown in Table 1 for an SNR of 40 dB. It is clear that the new algorithm has better performance than the others. Table 2 shows the results of the proposed algorithm where SNR varies from 40dB to 10dB. Obviously, the proposed algorithm is also robust to noise.

Table 5.1: A comparison of bias and variance of frequency estimation of the FM signal using different methods

SNR=40dB	Bias	Variance
energy operator	2.93×10^{-3}	3.31×10^{-3}
Hilbert Transform	2.84×10^{-3}	2.84×10^{-5}
TVAR with Chebyshev basis	2.20×10^{-5}	1.85×10^{-5}
proposed algorithm	1.10×10^{-5}	1.19×10^{-5}

Table 5.2: Bias and Variance of the frequency estimation of the FM signal using the proposed algorithm

SNR (dB)	Frequency estimation	
	Bias	Variance
40	1.10×10^{-5}	1.19×10^{-5}
30	3.92×10^{-5}	1.62×10^{-4}
20	1.41×10^{-3}	2.26×10^{-3}
10	1.33×10^{-1}	6.33×10^{-2}

5.2 Modeling and estimation of the real data

The real data sampled at Hong Kong harbor of China and Turbaden of Sweden with Hytec AB's ADCM-300 acoustic Doppler current profiler, have been used in testing the proposed algorithm. In the experiment, the ratios of the approximation error to signal are rather small, as 6.3% and 5.6%, respectively. This shows that TVAR(2) model is significantly coincident with the real backscattering signal. For example, figure. 5.1 shows the Hong Kong data and the corresponding modeling error of TVAR(2). Moreover, spectral centroid estimates using proposed algorithm are shown in figure 5.2 and 5.3, It should be noted that the purpose of showing these set of data is because the water current in HongKong harbor has more dynamic behavior than that of Turbaden. These two figures tell us: 1. spectral centroid estimate is not very sensitive to the predetermined bandwidth parameter d_t. 2. the wavelet shrinkage efficiently captured the inhomogeneous variations of the spectral centroid. 3. when the duration of the burst signal increase, the better frequency estimates are obtained. Finally, the appropriate choice of the wavelet shrinkage threshold will improve the results. In the above simulations, however, the universal threshold, $\sigma\sqrt{2log(nc)}$ (nc is the length of the wavelet coefficients), was used.

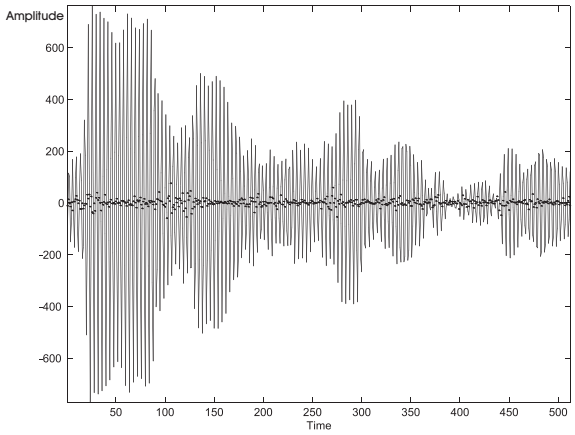

Figure 5.1: Signal sampled at Hong Kong Harbor, where solid line denotes the signal while dotted line denotes the approximation error of the TVAR(2).

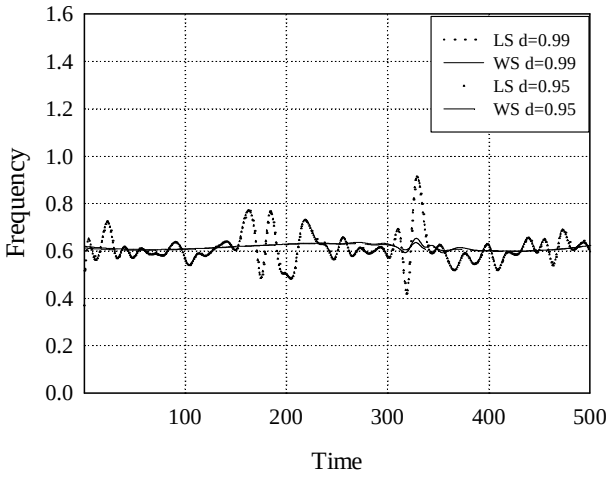

Figure 5.2: The spectral centroid estimates of the signal sampled at Hong Kong Harbor, where the duration is 461 circle. The LS denotes the least-square solution before wavelet shrinkage while WS denotes the after. d denotes the bandwidth setting.

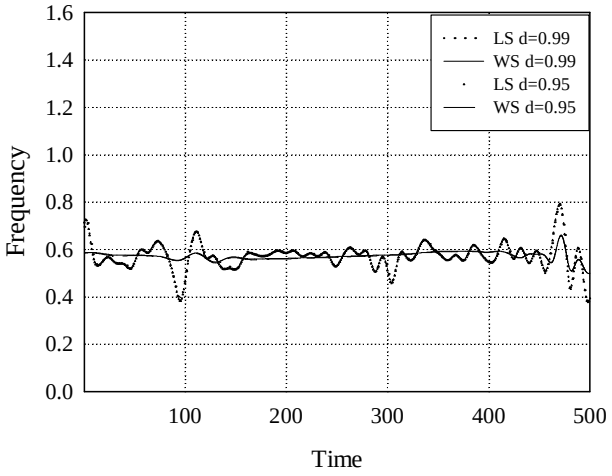

Figure 5.3: The spectral centroid estimates of the signal sampled at Hong Kong Harbor, where the duration is 923 circle. The LS denotes the least-square solution before wavelet shrinkage while WS denotes the after. d denotes the bandwidth setting.

Chapter 6

Discussion

This report has investigated the nonstationary statistical properties of the narrowband Doppler volume backscattering process. First, the mechanism of both finite duration Doppler effect and continuously space-shifted integration process was clarified. Then the signal model was formulated under the von Mises distribution assumption of the random phase. The first two order time-varying statistics expressions of the signal were derived. Moreover, based on the locally stationary process model, the evolutionary spectrum of the signal was obtained and its properties were analyzed. The last analysis was focused on the observability of the average flow speed by using the spectral centroid estimation. It has been shown that even under the ideally homogenous condition the spectral centroid intrinsically deviates from the average flow speed, due to the Doppler effect of a signal scatter and the density shift of the scatters. Finally, a semiparametric spectral centroid estimation method, which simply contains an AR(2) model with its time-varying coefficients adapted by a wavelet shrinkage, was proposed and numerically analyzed.

Appendix

Appendix A The first two order statistical structure

The backscattering signal component has the following form,

$$y(\omega_o, t) = 2\sqrt{\frac{v_s\omega_o}{\omega_s+\omega_o}}\int_{-\frac{T_o}{2}}^{\frac{T_o}{2}} A_{\omega_o,t-t'}\sin\left(\omega_o t' + \varphi_{t-t'}\right)dt'$$

where ω_o, T_o, and $\varphi_{t-t'}$ denotes frequency, duration and random phase, respectively. Note that $\omega_c T_c = \omega_o T_o = c$, due to finite duration Doppler effect. The random phase $\varphi_{t-t'}$ is assumed to obey a von Mises PDF as in equation (2.7). Let $\varphi_{_{t-t'}} = \psi_{_{t-t'}} + \bar{\varphi}_{_{t-t'}}$, where $\bar{\varphi}_{_{t-t'}}$ denotes the expected value of $\varphi_{_{t-t'}}$. Then $\psi_{t-t'}$ also has a von Mises distribution as,

$$f\left(\psi_{t-t'}\right) = \begin{cases} e^{\zeta_{t-t'}\cos\psi_{t-t'}}\left[2\pi I_0(\zeta_{_{t-t'}})\right]^{-1}, & |\psi_{t-t'}| \le \pi \\ 0, & |\psi_{t-t'}| > \pi \end{cases}$$

where $\zeta_{t-t'}$ is a real non-negative parameter. The modified Bessel function of various order is defined as, see 8.431.5 in [25],

$$I_k\left(\zeta_{t-t'}\right) = \frac{1}{\pi}\int_0^{\pi} e^{\zeta_{t-t'}\cos\psi_{t-t'}}\cos k\psi_{t-t'}d\psi_{t-t'}$$

where k is a non-negative integer. As $\cos\psi_{t-t'}$ and $e^{\zeta_{t-t'}\cos\psi_{t-t'}}$ are even functions while $\sin\psi_{t-t'}$ an odd one, we have,

$$\begin{aligned}
E(\sin\psi_{t-t'}) &= \frac{1}{2\pi I_0\left(\zeta_{t-t'}\right)}\int_{-\pi}^{\pi} e^{\zeta_{t-t'}\cos\psi_{t-t'}}\sin\psi_{t-t'}d\psi_{t-t'} = 0 \\
E(\sin 2\psi_{t-t'}) &= \frac{1}{2\pi I_0\left(\zeta_{t-t'}\right)}\int_{-\pi}^{\pi} e^{\zeta_{t-t'}\cos\psi_{t-t'}}\sin 2\psi_{t-t'}d\psi_{t-t'} = 0 \\
E(\cos\psi_{t-t'}) &= \frac{1}{2\pi I_0\left(\zeta_{t-t'}\right)}\int_{-\pi}^{\pi} e^{\zeta_{t-t'}\cos\psi_{t-t'}}\cos\psi_{t-t'}d\psi_{t-t'} = I_1(\zeta_{t-t'})I_0(\zeta_{t-t'})^{-1} \\
E(\cos 2\psi_{t-t'}) &= \frac{1}{2\pi I_0\left(\zeta_{t-t'}\right)}\int_{-\pi}^{\pi} e^{\zeta_{t-t'}\cos\psi_{t-t'}}\cos 2\psi_{t-t'}d\psi_{t-t'} = I_2(\zeta_{t-t'})I_0(\zeta_{t-t'})^{-1}
\end{aligned}$$

where $E[\cdot]$ denotes expected value. Then,

$$\begin{aligned} E\left[\sin\left(\omega_o t' + \varphi_{t-t'}\right)\right] &= E\left[\sin\left(\omega_o t' + \bar{\varphi}_{t-t'} + \psi_{t-t'}\right)\right] \\ &= \sin\left(\omega_o t' + \bar{\varphi}_{t-t'}\right) E\left[\cos\psi_{t-t'}\right] \\ &\quad + \cos\left(\omega_o t' + \bar{\varphi}_{t-t'}\right) E\left[\sin\psi_{t-t'}\right] \\ &= \sin\left(\omega_o t' + \bar{\varphi}_{t-t'}\right) I_1\left(\zeta_{t-t'}\right) I_0\left(\zeta_{t-t'}\right)^{-1} \end{aligned}$$

$$\begin{aligned} E\left[\cos\left(\omega_o t' + 2\varphi_{t-t'}\right)\right] &= E\left[\cos\left(\omega_o t' + 2\bar{\varphi}_{t-t'} + 2\psi_{t-t'}\right)\right] \\ &= \cos\left(\omega_o t' + 2\bar{\varphi}_{t-t'}\right) E\left[\cos 2\psi_{t-t'}\right] \\ &\quad - \sin\left(\omega_o t' + 2\bar{\varphi}_{t-t'}\right) E\left[\sin 2\psi_{t-t'}\right] \\ &= \cos\left(\omega_o t' + 2\bar{\varphi}_{t-t'}\right) I_2\left(\zeta_{t-t'}\right) I_0\left(\zeta_{t-t'}\right)^{-1} \end{aligned}$$

Let

$$\begin{aligned} \lambda_{t-t'} &= I_1\left(\zeta_{t-t'}\right) I_0\left(\zeta_{t-t'}\right)^{-1} \\ \kappa_{t-t'} &= 1 - \lambda_{t-t'}^2 \\ \rho_{t-t'} &= \lambda_{t-t'}^2 - I_2\left(\zeta_{t-t'}\right) I_0\left(\zeta_{t-t'}\right)^{-1}, \end{aligned}$$

then the mean is given as,

$$\begin{aligned} \bar{y}\left(\omega_o, t\right) &= E\left\{y\left(\omega_o, t\right)\right\} \\ &= E\left[2\sqrt{\frac{v_s\omega_o}{\omega_s+\omega_o}}\int_{-\frac{T_o}{2}}^{\frac{T_o}{2}} A_{\omega_o,t-t'}\sin\left(\omega_o t' + \varphi_{t-t'}\right)dt'\right] \\ &= 2\sqrt{\frac{v_s\omega_o}{\omega_s+\omega_o}}\int_{-\frac{T_o}{2}}^{\frac{T_o}{2}} A_{\omega_o,t-t'}\lambda_{t-t'}\sin\left(\omega_o t' + \bar{\varphi}_{t-t'}\right)dt' \qquad (6.1) \end{aligned}$$

Similarly, the second order statistics, i.e. covariance function, is written as,

$$\begin{aligned} &\operatorname{cov}\left[y\left(\omega_o, t-\frac{\tau}{2}\right), y\left(\omega_o, t+\frac{\tau}{2}\right)\right] \\ =\ & E\left\{\left[y\left(\omega_o, t-\frac{\tau}{2}\right) - \bar{y}\left(\omega_o, t-\frac{\tau}{2}\right)\right]\left[y(\omega_o, t+\frac{\tau}{2}) - \bar{y}(\omega_o, t+\frac{\tau}{2})\right]\right\} \\ =\ & E\left\{\int_{-\frac{T_o}{2}}^{\frac{T_o}{2}}\left[A_{\omega_o,t-\frac{\tau}{2}-t'}\sin\left(\omega_o t' + \varphi_{t-\frac{\tau}{2}-t'}\right) - A_{\omega_o,t-\frac{\tau}{2}-t'}\sin\left(\omega_o t' + \bar{\varphi}_{t-\frac{\tau}{2}-t'}\right)\lambda_{t-\frac{\tau}{2}-t'}\right]dt' \cdot \right. \\ & \left.\int_{-\frac{T_o}{2}}^{\frac{T_o}{2}}\left[A_{\omega_o,t+\frac{\tau}{2}-t''}\sin\left(\omega_o t'' + \varphi_{t+\frac{\tau}{2}-t''}\right) - A_{\omega_o,t+\frac{\tau}{2}-t''}\sin\left(\omega_o t'' + \bar{\varphi}_{t+\frac{\tau}{2}-t''}\right)\lambda_{t+\frac{\tau}{2}-t''}\right]dt''\right\} \cdot \\ & \frac{4v_s\omega_o}{\omega_s+\omega_o} \end{aligned}$$

$$
\begin{aligned}
&= \int_{-\frac{T_o}{2}}^{\frac{T_o}{2}} \int_{-\frac{T_o}{2}}^{\frac{T_o}{2}} E\left\{\left[A_{\omega_o,t-\frac{\tau}{2}-t'} \sin\left(\omega_o t' + \varphi_{t-\frac{\tau}{2}-t'}\right) - A_{\omega_o,t-\frac{\tau}{2}-t'} \sin\left(\omega_o t' + \bar{\varphi}_{t-\frac{\tau}{2}-t'}\right) \lambda_{t-\frac{\tau}{2}-t'}\right] \cdot \right. \\
&\quad \left. \left[A_{\omega_o,t+\frac{\tau}{2}-t''} \sin\left(\omega_o t'' + \varphi_{t+\frac{\tau}{2}-t''}\right) - A_{\omega_o,t+\frac{\tau}{2}-t''} \sin\left(\omega_o t'' + \bar{\varphi}_{t+\frac{\tau}{2}-t''}\right) \lambda_{t+\frac{\tau}{2}-t''}\right]\right\} dt' dt'' \cdot \\
&\quad \frac{4 v_s \omega_o}{\omega_s + \omega_o}
\end{aligned}
$$

In the above expression, the last expectation term will become zero if $t' + \frac{\tau}{2} \neq t'' - \frac{\tau}{2}$. Otherwise,

$$
\begin{aligned}
&\operatorname{cov}\left[y\left(\omega_o, t - \frac{\tau}{2}\right), y\left(\omega_o, t + \frac{\tau}{2}\right)\right] \\
&= \int_{-\frac{T_o-|\tau|}{2}}^{\frac{T_o-|\tau|}{2}} A^2_{\omega_o,t-t'} E\left\{\left[\sin\left(\omega_o t' - \omega_o \frac{|\tau|}{2} + \varphi_{t-t'}\right) - \sin\left(\omega_o t' - \omega_o \frac{|\tau|}{2} + \bar{\varphi}_{t-t'}\right) \lambda_{t-t'}\right] \cdot \right. \\
&\quad \left. \left[\sin\left(\omega_o t' + \omega_o \frac{|\tau|}{2} + \varphi_{t-t'}\right) - \sin\left(\omega_o t' + \omega_o \frac{|\tau|}{2} + \bar{\varphi}_{t-t'}\right) \lambda_{t-t'}\right]\right\} dt' \frac{4 v_s \omega_o}{\omega_s + \omega_o}
\end{aligned}
$$

If $\tau \notin [-T_o, T_o]$, the above formula equals to zero. When $\tau \in [-T_o, T_o]$,

$$
\begin{aligned}
&\operatorname{cov}\left[y\left(\omega_o, t - \frac{\tau}{2}\right), y\left(\omega_o, t + \frac{\tau}{2}\right)\right] \\
&= \int_{-\frac{T_o-|\tau|}{2}}^{\frac{T_o-|\tau|}{2}} A^2_{\omega_o,t-t'} E\left[\sin\left(\omega_o t' - \omega_o \frac{|\tau|}{2} + \varphi_{t-t'}\right) \sin\left(\omega_o t' + \omega_o \frac{|\tau|}{2} + \varphi_{t-t'}\right)\right] \\
&\quad - A^2_{\omega_o,t-t'} \sin\left(\omega_o t' - \omega_o \frac{|\tau|}{2} + \bar{\varphi}_{t-t'}\right) \sin\left(\omega_o t' + \omega_o \frac{|\tau|}{2} + \bar{\varphi}_{t-t'}\right) \lambda^2_{t-t'} dt' \frac{4 v_s \omega_o}{\omega_s + \omega_o} \\
&= \int_{-\frac{T_o-|\tau|}{2}}^{\frac{T_o-|\tau|}{2}} \left\{A^2_{\omega_o,t-t'} E\left[\cos \omega_o |\tau| - \cos\left(2\omega_o t' + 2\varphi_{t-t'}\right)\right]\right. \\
&\quad \left. - A^2_{\omega_o,t-t'} \left[\cos \omega_o |\tau| - \cos\left(2\omega_o t' + 2\bar{\varphi}_{t-t'}\right)\right] \lambda^2_{t-t'}\right\} dt' \frac{2 v_s \omega_o}{\omega_s + \omega_o} \\
&= \cos\left(\omega_o |\tau|\right) \int_{-\frac{T_o-|\tau|}{2}}^{\frac{T_o-|\tau|}{2}} A^2_{\omega_o,t-t'} \kappa_{t-t'} dt' \frac{2 v_s \omega_o}{\omega_s + \omega_o} \\
&\quad + \int_{-\frac{T_o-|\tau|}{2}}^{\frac{T_o-|\tau|}{2}} A^2_{\omega_o,t-t'} \rho_{t-t'} \cos\left(2\omega_o t' + 2\bar{\varphi}_{t-t'}\right) dt' \frac{2 v_s \omega_o}{\omega_s + \omega_o}. \qquad (6.2)
\end{aligned}
$$

Appendix B A spectral expression

Given a real valued function $x(t)$ with DC component $\bar{x}$, a real even signal $y(\tau)$ is written as,

$$y(\tau) = \begin{cases} \int_{\frac{-T+\tau}{2}}^{\frac{T-\tau}{2}} x(t)\,dt & \tau \in [0,T], \\ \int_{\frac{-T-\tau}{2}}^{\frac{T+\tau}{2}} x(t)\,dt & \tau \in [-T,0], \\ 0 & otherwise. \end{cases}$$

When $\tau \in [0,T]$,

$$\begin{aligned} y(\tau) &= \int_{\frac{-T+\tau}{2}}^{\frac{T-\tau}{2}} x(t)\,dt \\ &= \frac{1}{2}\int_{-T+\tau}^{0} x\left(\frac{t}{2}\right)dt + \frac{1}{2}\int_{0}^{T-\tau} x\left(\frac{t}{2}\right)dt \\ &= \frac{1}{2}\int_{\tau-T}^{0} x\left(\frac{t}{2}\right) + x\left(\frac{-t}{2}\right)dt \\ &= \frac{1}{2}\int_{-T}^{0}\left[x\left(\frac{t}{2}\right) + x\left(\frac{-t}{2}\right)\right]\left[u(\tau-t) - u(\tau-t-T)\right]dt \end{aligned}$$

where $u(\tau)$ denotes the step function. Let

$$\tilde{x}(t) = x(t) - \bar{x}$$

We have the spectrum representation of $y(\tau)$ as,

$$\begin{aligned} f_y(\omega) &= 2\mathrm{Re}\left\{\int_0^\infty y(\tau)\,e^{-i\omega\tau}d\tau\right\} \\ &= \mathrm{Re}\left\{\int_0^\infty\int_{-T}^{0}\left[x\left(\frac{t}{2}\right) + x\left(\frac{-t}{2}\right)\right]\left[u(\tau-t) - u(\tau-t-T)\right]dte^{-i\omega\tau}d\tau\right\} \\ &= \mathrm{Re}\left\{\int_{-\infty}^{0}\left[x\left(\frac{t}{2}\right) + x\left(\frac{-t}{2}\right)\right]\int_0^\infty\left[u(\tau-t) - u(\tau-t-T)\right]e^{-i\omega\tau}d\tau dt\right\} \\ &= \mathrm{Re}\left\{\int_{-T}^{0}\left[x\left(\frac{t}{2}\right) + x\left(\frac{-t}{2}\right)\right]\int_0^{t+T} e^{-i\omega\tau}d\tau dt\right\} \\ &= \mathrm{Re}\left\{\int_{-T}^{0}\left[x\left(\frac{t}{2}\right) + x\left(\frac{-t}{2}\right)\right]\frac{e^{-i\omega(t+T)}-1}{-i\omega}dt\right\} \\ &= \int_{-T}^{0}\left[x\left(\frac{t}{2}\right) + x\left(\frac{-t}{2}\right)\right]\frac{\sin\omega(t+T)}{\omega}dt \\ &= \int_{-\frac{T}{2}}^{0} 2\left[x(t) + x(-t)\right]\frac{\sin\omega(2t+T)}{\omega}dt \end{aligned}$$

$$
\begin{aligned}
&= 4\bar{x}\int_{-\frac{T}{2}}^{0}\frac{\sin\omega\left(2t+T\right)}{\omega}dt+\int_{-\frac{T}{2}}^{0}2\left[\tilde{x}\left(t\right)+\tilde{x}\left(-t\right)\right]\frac{\sin\omega\left(2t+T\right)}{\omega}dt\\
&= \bar{x}T^{2}\mathrm{sinc}^{2}\frac{\omega T}{2}+2\int_{-\frac{T}{2}}^{0}\left[x\left(t\right)+x\left(-t\right)\right]\frac{\sin 2\omega t\cos\omega T+\cos 2\omega t\sin\omega T}{\omega}dt\\
&= \bar{x}T^{2}\mathrm{sinc}^{2}\frac{\omega T}{2}+2\frac{\cos T\omega}{\omega}\int_{-\frac{T}{2}}^{0}\left[x\left(t\right)+x\left(-t\right)\right]\sin 2\omega t dt\\
&\quad +2\frac{\sin T\omega}{\omega}\int_{-\frac{T}{2}}^{0}\left[x\left(t\right)+x\left(-t\right)\right]\cos 2\omega t dt
\end{aligned}
$$

Acknowledgement

The authors wish to express their gratitude to Department of Telecommunications and Signal Processing for providing a patient support and a pleasant scientific research environment during the years. Especially we would like to thank Timothy Samuels and Dr. Abbas Mohammed for their expert help and constructive comments on the manuscript at various stages. We take this opportunity to thank Dr. Thomas Lagö and Dr. Per Ericsson for their invaluable management of the hydroacoustic project.

Bibliography

[1] R. J. Urick, *Principles of Underwater Sound,* 3d ed. New York: Mcgraw-Hill, 1983.

[2] C. Clay and H. Medwin, *Acoustical Oceanography: principles and applications,* John Wiley, 1977.

[3] A. Pierce, *Acoustics,* The Acoustical Society of America, 1981.

[4] P. M. Morse and K. Uno Ingard, *Theoretical Acoustics,* Princeton University Press, 1986.

[5] *IEEE J. Oceanic Eng.*, vol. 11, no. 1, 1986.

[6] G. Appell and T. Curtin ed., A special issue on current measurement, *IEEE J. Oceanic Eng.*, vol. 16, no. 4, 1991.

[7] A. J. Williams, "Current measurement technology development progress in the '90s - a review," *Proc. Oceans '96*, MTS/IEEE, pp. 105-109, Sept. 1996.

[8] M. F. Insana, R. F. Wagner, D. G. Brown and T. J. Hall, "Describing small-scale structure in random media using pulse-echo ultrasound," *Journal of Acoustical Society of America*, vol. 87, pp. 179-192, Jan. 1990.

[9] J. W. Goodman, *Statistical Optics*, New York: John Wiley and sons, 1985.

[10] S. O. Rice, "Mathematical analysis of random noise," *Bell Systems Technial Journal*, vol. 14, pp. 46-158, 1945.

[11] T. A. Tuthill, R. H. Sperry and K. J. Parker, "Deviation from Rayleigh statistics in ultrasonic speckle," *Ultrasonic Imaging*, vol. 10, pp. 81-90, Apr. 1988.

[12] E. Jakeman and P. N. Pusey, "A model for non-Rayleigh sea echo," *IEEE Trans. Antennas and Propagation*, vol. 24, pp. 806-814, 1976.

[13] V. Dutt, "Statistical analysis of ultrasonic echo envelope," Ph. D Thesis, Mayo Graduate school, Aug. 1995.

[14] R. Dahlhaus, "Fitting time series models to nonstationary processes," *Annal. Statist.*, vol. 25, no. 1, 1997.

[15] R. Dahlhaus, M. Neumann and R. von Sachs, "Nonlinear wavelet estimation of time-varying autoregressive process," *Berichte der AG Technomathematik* 145, Universitaet Kaiserslautern. to appear in *Bernoulli*, vol. 5, no. 5, 1999.

[16] S. Mukhopadhyay and P. Sircar, "Parametric modelling of non-stationary signals: A unified approach," *Signal Processing*, vol. 60, pp. 135-152, 1997.

[17] J. Rajan and P. Rayner, "Generalized Feature Extraction for Time-Varying Autoregressive Models," *IEEE Trans. Signal Processing*, vol. 44, no. 10, pp. 2498-2507, 1996.

[18] S. M. Kay, "Accurate frequency estimation at low signal-to-noise ratio," *IEEE Trans. Acoust., Speech, Signal Processing*, vol. 32, no. 3, pp. 540-547, 1984.

[19] T. H. Li and B. Kedem, "Iterative filtering for multiple frequency estimation," *IEEE Trans. Signal Processing*, vol. 42, no. 5, pp. 1120-1132, 1994.

[20] B. Truong-Van, "A new approach to frequency analysis with amplified harmonics," *J. R. Statist. Soc.*, B 52, pp. 203-221, 1990.

[21] D. Donoho, I. Johnstone, G. Kerkyacharian and D. Picard, "Wavelet shrinkage: asymptopia? (with discussion)," *J. R. Statist. Soc.*, B 57, pp. 301-369, 1995.

[22] A. Potaminanos, and P. Maragos, "A comparison of energy operators and the Hilbert transform approach to signal and speech demodulation," *Signal Processing*, vol. 37, no. 1, 1994.

[23] A. Cohen, I. Daubechies, B. Jawerth and P. Vial, "Multiresolution analysis, wavelets and fast algorithms on an interval," *Comptes Rendus Acad. Sc. Paris* 316 (serie I) pp. 417-421, 1993

[24] A. Cohen, *Time-Frequency Signal Analysis*, Englewood Cliffs, NJ: Prentice Hall, 1995.

[25] I. S. Gradshteyn, I. M. Ryzhik, *Tabel of Integrals, Series and Products: Cd-Rom Version 1.0*, Academic Press, 1996

[26] A. Gupta, "Variance expressions for four spectral-centroid estimators of a complex Gaussian process," *IEEE Trans. Inform. Theory*, vol. 32, no. 11, pp. 73-78, Jan. 1984.

[27] G. Jacovitti and R. Cusani, "Performance of normalized correlation estimators for complex processes," *IEEE Trans. Signal Processing*, vol. 40, no. 1 pp. 114-128, Jan. 1992